Polymer Journal, Vol. 36, No. 12, pp. 971—978 (2004)

Variation in Size and Shape of Hexaoxyethylene Dodecyl Ether $C_{12}E_6$ Micelles with Uptake of *n*-Dodecane and *n*-Dodecanol in Dilute Aqueous Solution

Yoshiyuki EINAGA,† Yukari TOTAKE, and Hiroko MATSUYAMA

Department of Chemistry, Nara Women's University, Kitauoya Nishi-machi, Nara 630-8506, Japan

(Received July 22, 2004; Accepted September 7, 2004; Published December 15, 2004)

ABSTRACT: The size and shape of hexaoxyethylene dodecyl ether $C_{12}E_6$ micelles in dilute aqueous solutions with oil (*n*-dodecane and *n*-dodecanol) uptake were investigated by static (SLS) and dynamic light scattering (DLS) experiments at 40.0 °C for the $C_{12}E_6$ + water + *n*-dodecane system and at 25.0 °C for the $C_{12}E_6$ + water + *n*-dodecanol system. The micelles collapse into the smaller ones by incorporating *n*-dodecane, implying that the incorporation of the oil weakens hydrophilic interactions among polyoxyethylene tail of the surfactant molecules and water too significantly to maintain the original micellar size. The inclusion of *n*-dodecanol causes growth in the micellar size, suggesting that *n*-dodecanol plays a role as a kind of co-surfactant. Accompanying size change, the micelles were found to alter their shape from the original wormlike shape to prolate ellipsoid with the oil uptake. The axial ratios determined are 17.4 and 9.2 for micelles containing *n*-dodecane and *n*-dodecanol, respectively. The volume allotted to each $C_{12}E_6$ molecule (including the oil) in the micelles does not vary much with oil content. [DOI 10.1295/polymj.36.971]

KEY WORDS Polyoxyethylene Alkyl Ether / Micelle / Phase Diagram / Static Light Scattering / Dynamic Light Scattering / Diffusion Coefficient / Hydrodynamic Radius /

Non-ionic surfactant polyoxyethylene alkyl ether C_iE_j forms polymer-like or wormlike micelles in dilute aqueous solutions (L_1 phase).[1–14] Here, *i* and *j* are the numbers of methylene and oxyethylene groups, respectively. The micelles grow in size with increasing surfactant concentration and raising temperature toward the lower consolute phase boundary. In the preceding paper,[15] we determined shape, size, and weight-average molar mass M_w of the $C_{12}E_6$ and $C_{14}E_6$ micelles by static (SLS) and dynamic light scattering (DLS). The characterization of individual "isolated"micelles of $C_{12}E_6$ and $C_{14}E_6$ free from intermicellar interactions at finite surfactant concentrations was done with the aid of the thermodynamic theory for SLS of micellar solutions.[16] Extrapolations of the SLS and DLS results to infinite dilution yield the data set representing the relationships between the hydrodynamic radius R_H and M_w for the isolated micelles in dilute solutions.

The size and shape of the C_iE_j micelles vary with uptake of oils into the cylindrical micelles. Menge *et al.*[17–19] investigated the effects of added oil on the structure of the micelles in the L_1 phase of the system $C_{12}E_5$ + water + decane by SLS, DLS, and small-angle neutron scattering (SANS) measurements. They showed that at overall concentrations of $C_{12}E_5$ + decane up to *ca.* 0.100 g/cm^3, the (apparent) molar mass of the micelles gradually increases with decane content up to the decane mass fraction of *ca.* 0.07–0.10, and then sharply decreases with further increase of decane content. The micelles at low decane and $C_{12}E_5$ + decane concentrations may be represented with a wormlike polymer model, but at high decane contents, the micelles eventually become microemulsion droplets whose shapes are not necessarily spherical. Variation in micellar shape with oil uptake has been also observed directly by cryogenic temperature transmission electron microscopy (cryo-TEM) for the system $C_{12}E_5$ + water + *n*-octane.[20]

Kunieda *et al.*[21,22] studied the size evolution of the $C_{12}E_5$, $C_{12}E_6$, $C_{12}E_7$, and $C_{12}E_9$ micelles with addition of poly(isoprene)–poly(oxyethylene) diblock copolymer (PI–PEO or $C_{250}E_{70}$) by DLS measurements. Their results reveal that the (apparent) hydrodynamic radius $R_{H,app}$ of the $C_{12}E_5$ micelles becomes smaller at low PI–PEO content up to weight fraction of 0.2, passes through a minimum, and then increases with increasing PI–PEO content. The sizes of the $C_{12}E_6$, $C_{12}E_7$, and $C_{12}E_9$ micelles at small PI–PEO contents have been found not to change upon addition of PI–PEO, although the $C_{12}E_6$ micelles grow in size with further addition of PI–PEO similarly as in the case of the $C_{12}E_5$ micelles at high PI–PEO contents. The authors conjecture that the micelles assume rodlike shape and their lengths become shorter as the number *j* becomes larger, thereby explaining the observed phenomena.

The present work first examines phase behavior of the ternary systems $C_{12}E_6$ + water + *n*-dodecane and $C_{12}E_6$ + water + *n*-dodecanol, and then characteriz-

†To whom correspondence should be addressed (E-mail: einaga@cc.nara-wu.ac.jp).

es micelles formed in the L_1 phase of these systems. In the characterization, relationships between molar mass M_w and hydrodynamic radius R_H of the micelles free from intermicellar thermodynamic and hydrodynamic interactions were determined on the basis of the findings given in the previous paper.[15]

EXPERIMENTAL

Materials

High-purity $C_{12}E_6$ sample was purchased from Nikko Chemicals Co., Ltd. and used without further purification. *n*-Dodecane and *n*-dodecanol were from Nakaraitesque Co. and used as delivered. The solvent water used was of high purity (ultrapure) and prepared with Simpli Lab water purification system of Millipore Co.

Phase Diagram

Cloud-point temperatures of given test solutions were determined visually as temperatures at which originally transparent solutions became turbid when temperature was gradually raised.

$C_{12}E_6$ micelle solutions were prepared by dissolving $C_{12}E_6$ in water with adding appropriate amounts of *n*-dodecane or *n*-dodecanol with a microliter syringe (Hamilton). Complete mixing and micelle formation were achieved by stirring using a magnetic stirrer at least one day. Both *n*-dodecane and *n*-dodecanol are insoluble in water and thus are completely incorporated into the micelles. The weight fractions w of micelle solutions were determined gravimetrically and converted to mass concentrations c by the densities ρ of the solutions given below. Throughout this paper, w and c denote the weight fraction and mass concentration of $C_{12}E_6$ + *n*-dodecane (or *n*-dodecanol) in the $C_{12}E_6$ + water + *n*-dodecane (or *n*-dodecanol) ternary solutions. *n*-Dodecane (or *n*-dodecanol) content is represented by its weight fraction w_d in the $C_{12}E_6$ + *n*-dodecane (or *n*-dodecanol) mixtures.

Static Light Scattering

SLS measurements were performed to obtain the weight-average molar mass M_w of the micelles at 40.0 °C for the $C_{12}E_6$ + water + *n*-dodecane solutions and at 25.0 °C for the $C_{12}E_6$ + water + *n*-dodecanol solutions. The apparatus used is an ALV DLS/SLS-5000/E light scattering photogoniometer and correlator system with vertically polarized incident light of 632.8 nm wavelength from a Uniphase Model 1145P He–Ne gas laser. For calibration of the apparatus, the intensity of light scattered from pure benzene was measured at 25.0 °C at a scattering angle of 90°, where the Rayleigh ratio R_{Uv} (90) of pure benzene for unpolarized scattered light with polarized incident light at a wavelength of 632.8 nm was taken as 11.84×10^{-6} cm^{-1}.[23,24]

The micelle solutions were prepared in the same way as in the case of cloud-point measurements. The solutions prepared were optically purified by filtration through a membrane of 0.20 μm pore size.

Scattering intensity was measured for each solution and for the solvent water at scattering angles θ ranging from 30 to 150°. From the excess Rayleigh ratio ΔR_0 extrapolated to zero scattering angle for a given solution, we evaluated M_w by

$$\frac{Kc}{\Delta R_0} = \frac{1}{M_w} + 2A_2c + \cdots \tag{1}$$

where A_2 is the second virial coefficient and K is the optical constant defined as

$$K = \frac{4\pi^2 n^2 (\partial n/\partial c)_{T,p}^2}{N_A \lambda_0^4} \tag{2}$$

with N_A Avogadro's number, λ_0 the wavelength of the incident light at vacuum, n and $(\partial n/\partial c)_{T,p}$ the refractive index and the refractive index increment of the solution, T the absolute temperature and p the pressure. In the present case, M_w is, in general, a function of concentration c. We treat solutions consisting of $C_{12}E_6$, water, and *n*-dodecane (or *n*-dodecanol) as substantially binary systems by taking $C_{12}E_6$ micelles including *n*-dodecane (or *n*-dodecanol) as solute components.

$(\partial n/\partial c)_{T,p}$ at 632.8 nm was measured at 20.0, 30.0, and 40.0 °C for the $C_{12}E_6$ + water + *n*-dodecane solutions and at 25.0, 30.0, and 35.0 °C for the $C_{12}E_6$ + water + *n*-dodecanol solutions with a Union Giken R601 differential refractometer. The results for the former solutions are given as

$$(\partial n/\partial c)_{T,p} = A - 3 \times 10^{-4} w_d \tag{3}$$

where A at 20.0, 30.0, and 40.0 °C were 0.1318, 0.1279, and 0.1275, respectively. $(\partial n/\partial c)_{T,p}$ of the latter solutions was almost independent of w_d and 0.1281, 0.1268, and 0.1255 at 25.0, 30.0, and 35.0 °C, respectively.

Dynamic Light Scattering

DLS measurements were carried out to determine the translational diffusion coefficient D of the micelles at 40.0 °C for the $C_{12}E_6$ + water + *n*-dodecane solutions and at 25.0 °C for the $C_{12}E_6$ + water + *n*-dodecanol solutions by the use of the same apparatus and light source as used in the SLS studies described above. The normalized autocorrelation function $g^{(2)}(t)$ of scattered light intensity $I(t)$, *i.e.*,

$$g^{(2)}(t) = \langle I(0)I(t)\rangle / \langle I(0)\rangle^2 \tag{4}$$

was measured at scattering angles θ ranging from 30 to 150°.

All test solutions are the same as those used in the SLS studies. From the data for $g^{(2)}(t)$, we determined D by the equation

$$(1/2)\ln[g^{(2)}(t) - 1] = (1/2)\ln f - K_1 t + \cdots \quad (5)$$

$$D = \lim_{q \to 0} K_1/q^2 \quad (6)$$

Here, f is the coherent factor fixed by the optical system, K_1 is the first cumulant, and q is the magnitude of the scattering vector defined by

$$q = \frac{4\pi n}{\lambda_0} \sin\left(\frac{\theta}{2}\right) \quad (7)$$

D should be regarded as the z-average, since the micelles may have distribution in size.

Density

The solution density ρ required for calculation of c was measured at 25.0, 30.0, and 35.0 °C for both the $C_{12}E_6$ + water + *n*-dodecane and $C_{12}E_6$ + water + *n*-dodecanol solutions with a pycnometer of the Lipkin–Davison type. ρ of the two micelle solutions at each temperature was independent of surfactant concentration and *n*-dodecane (or *n*-dodecanol) content in the range of concentration examined.

$$\rho = 1.00470 - 3.305 \times 10^{-4}(T - 273.15) \quad (8)$$

for the former system, and

$$\rho = 1.00457 - 3.160 \times 10^{-4}(T - 273.15) \quad (9)$$

for the latter. Partial specific volume v of the micelles was calculated as ρ^{-1}, since ρ is independent of micelle concentration.

RESULTS

Phase Behavior

In Figure 1, cloud point curves are depicted for ternary systems $C_{12}E_6$ + water + *n*-dodecane and $C_{12}E_6$ + water + *n*-dodecanol at various w_d indicated. Here, the data points for the binary system $C_{12}E_6$ + water are the literature results by Yoshimura *et al.* (large filled circles)[15] and Briganti *et al.* (small filled circles)[25] Figure 2 illustrates three-dimensional representations of the binodal surfaces for the same ternary systems as those in Figure 1 constructed from the cloud point data. The cloud point curve for each w_d is the intersection of the binodal surface by the constant solute (micelle) composition, or constant *n*-dodecane or *n*-dodecanol content w_d, on which the composition of a given solute mixture is fixed but the temperature and overall solute concentration w in solution are varied.

For both ternary systems, L_1 phases are formed at low temperatures and the solutions are phase-separated with raising temperature, showing LCST (lower critical solution temperature) behavior. In the case of the $C_{12}E_6$ + water + *n*-dodecane system, the cloud point temperature at fixed w decreases with w_d at small w_d, passes through a minimum, and then increases as w_d is increased. The cloud point temperature of the $C_{12}E_6$ + water + *n*-dodecanol solutions of a given w continually decreases with increasing w_d. The results for the phase behavior suggest that change in size or shape of the micelles with uptake of *n*-dodecane and *n*-dodecanol into them is greatly different in the two systems.

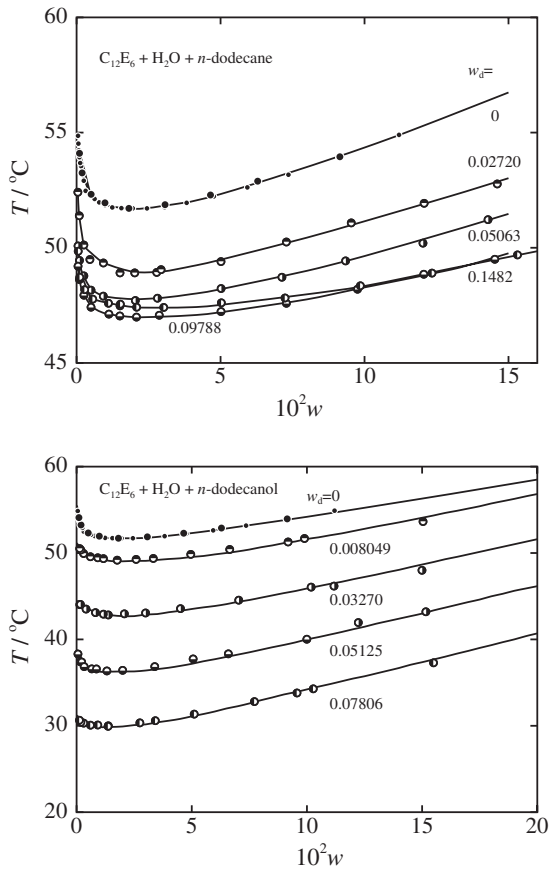

Figure 1. Cloud point curves for $C_{12}E_6$ + water + *n*-dodecane and $C_{12}E_6$ + water + *n*-dodecanol solutions at various w_d. The data points for $w_d = 0$ are literature results by Yoshimura *et al.*[15] (large circles) and Briganti *et al.*[25] (small circles).

Static Light Scattering

In Figure 3, $Kc/\Delta R_0$ for all micelle solutions examined at various w_d are plotted in the form of $(Kc/\Delta R_0)^{1/2}$ against the solute mass concentration c. For the $C_{12}E_6$ + water + *n*-dodecane system, $(Kc/\Delta R_0)^{1/2}$ does not vary to a great extent with c and w_d, although its w_d dependence is somewhat complicated, while $(Kc/\Delta R_0)^{1/2}$ of the $C_{12}E_6$ + water + *n*-dodecanol solutions at any fixed c continuously decreases with w_d. The c dependence of $Kc/\Delta R_0$ may be

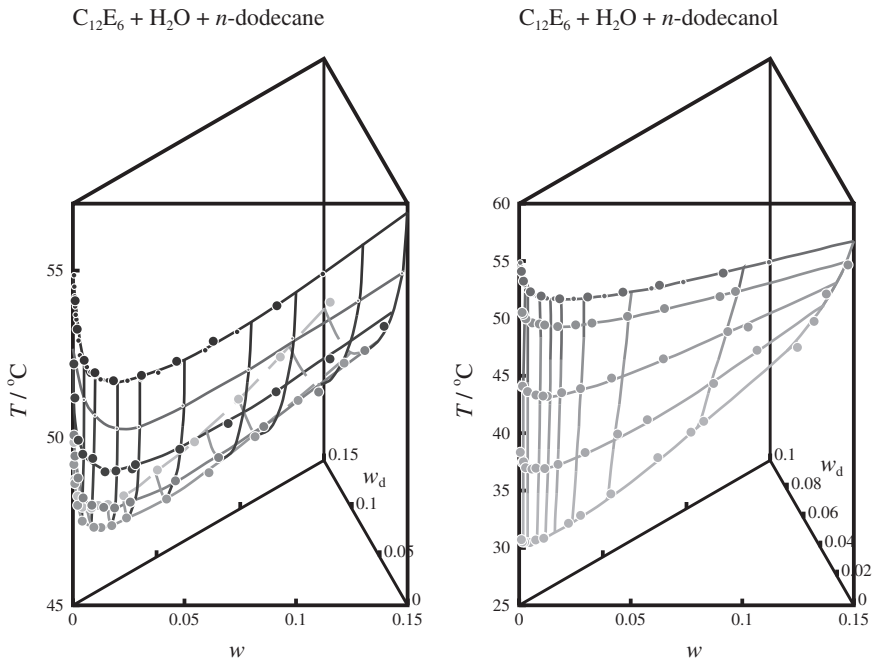

Figure 2. Three-dimensional representation of the binodal surface for $C_{12}E_6$ + water + *n*-dodecane and $C_{12}E_6$ + water + *n*-dodecanol solutions. Filled circles: experimental cloud point data. The data points for $w_d = 0$ are the literature results by Yoshimura *et al.*[15] (large circles) and Briganti *et al.*[25] (small circles).

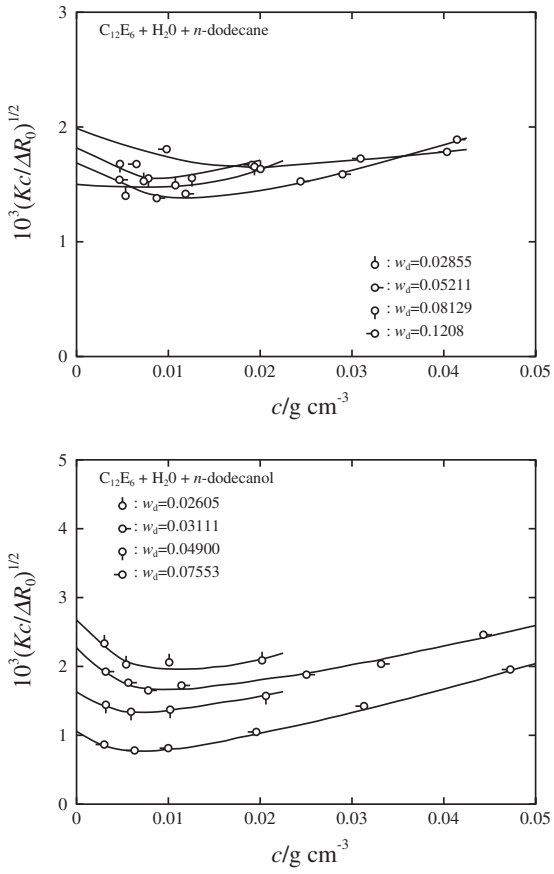

Figure 3. Plots of $(Kc/\Delta R_0)^{1/2}$ against c for $C_{12}E_6$ + water + *n*-dodecane solutions at 40.0 °C and for $C_{12}E_6$ + water + *n*-dodecanol solutions at 25.0 °C at various w_d indicated.

interpreted in terms of the polymer solution theory represented by eq 1. The molar mass M_w of the micelle may vary with concentration c in the case of micelle solutions, being different from the case of polymer solutions. Thus, c dependence of $(Kc/\Delta R_0)^{1/2}$ found in Figure 3 does not necessarily reflect only the values of virial coefficients such as A_2 and so on, but possibly includes the effects of concentration-dependent increase of M_w. It is rather challenging to evaluate these two effects separately. In the present work, we determined M_w from the ordinate intercepts by extrapolating the data points at a given w_d to infinite dilution following the lines shown in the figures. The previous work[15] indicated that this procedure may yield M_w of the micelles free from intermicellar interactions, *i.e.*, it can successfully eliminate the effects of the second and higher virial coefficient terms on $(Kc/\Delta R_0)^{1/2}$.

M_w thus obtained are listed in Tables I and II, and plotted against w_d in Figure 4, where the values at $w_d = 0$ (filled circles) are the results for the binary system $C_{12}E_6$ + water obtained previously.[15] From Figure 3, $C_{12}E_6$ micelles disintegrate with addition of *n*-dodecane to the micelle solution, while the addition of *n*-dodecanol causes growth in micellar size.

Dynamic Light Scattering

Figure 5 shows D as a function of c for all micelle solutions at various w_d. When compared at fixed c, D of the $C_{12}E_6$ micelle including *n*-dodecane increases

Table I. M_w and R_H for Micelles in the System $C_{12}E_6$ + water + *n*-dodecane at 40.0 °C

$10^{-4}M_w$	R_H (nm)	b (nm)
59.7	15.0	
44.4	10.5	2.16
35.2	9.82	2.00
30.3	9.33	1.90
25.3	8.87	1.79

Table II. M_w and R_H for Micelles in the System $C_{12}E_6$ + water + *n*-dodecanol at 25.0 °C

$10^{-4}M_w$	R_H (nm)	b (nm)
6.0	3.72	
14.0	5.99	1.82
19.5	6.62	2.03
37.8	7.61	2.54
89.6	10.7	3.38

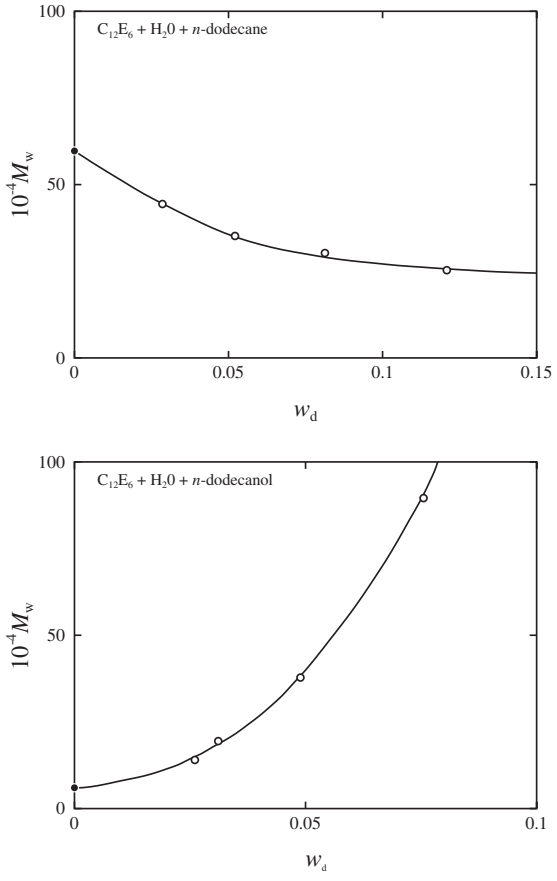

Figure 4. Plots of M_w against w_d for $C_{12}E_6$ + water + *n*-dodecane solutions at 40.0 °C and for $C_{12}E_6$ + water + *n*-dodecanol solutions at 25.0 °C: Unfilled circles, present data; Filled circles, previous results for the $C_{12}E_6$ + water binary system.[15]

with w_d, while that of the $C_{12}E_6$ micelle including *n*-dodecanol decreases with w_d. At any given w_d, D decreases with c at small c and then becomes approximately constant at higher c. The c dependence of D reflects not only variation of micellar size with c but the effects of intermicellar thermodynamic and hydrodynamic interactions. As in the case of the SLS, we extrapolated the data points at a given w_d to infinite dilution following the curve shown in the figures, in order to eliminate the latter effects on the basis of the findings given in the previous paper.[15] From extrapolated D, the hydrodynamic radius R_H of the micelles defined according to the Stokes–Einstein relation

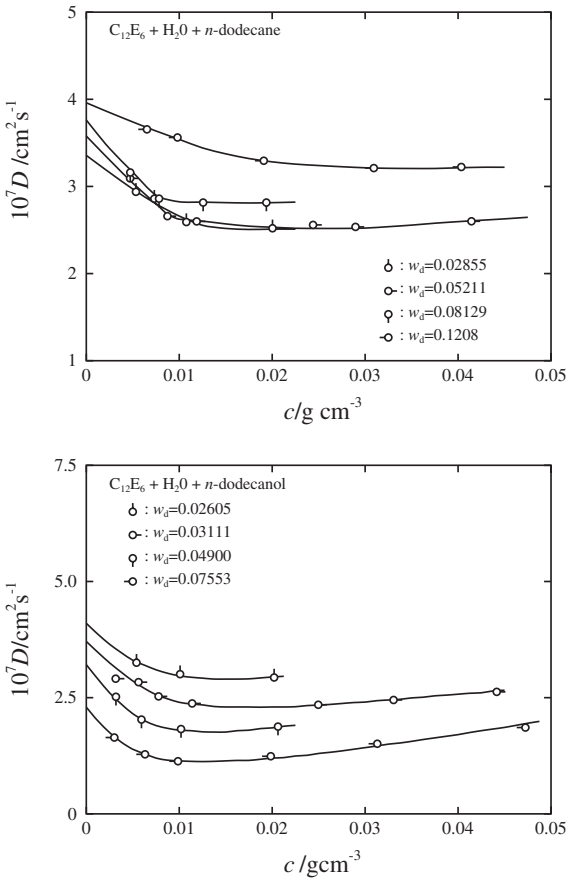

Figure 5. Plots of D against c for $C_{12}E_6$ + water + *n*-dodecane solutions at 40.0 °C and for $C_{12}E_6$ + water + *n*-dodecanol solutions at 25.0 °C at various w_d indicated.

$$D = \frac{k_B T}{6\pi\eta_0 R_H} \tag{10}$$

was calculated. Here, k_B is the Boltzmann constant and η_0 is solvent viscosity. The previous results[15] for $C_{12}E_6$ and $C_{14}E_6$ micelles show that R_H obtained in this way as a function of M_w is in good agreement with that for the "isolated" micelles determined by a theory at finite concentrations.

R_H thus obtained for the $C_{12}E_6$ + *n*-dodecane and $C_{12}E_6$ + *n*-dodecanol micelles are summarized in Tables I and II, respectively, along with those of M_w and are plotted against w_d in Figure 6, where the val-

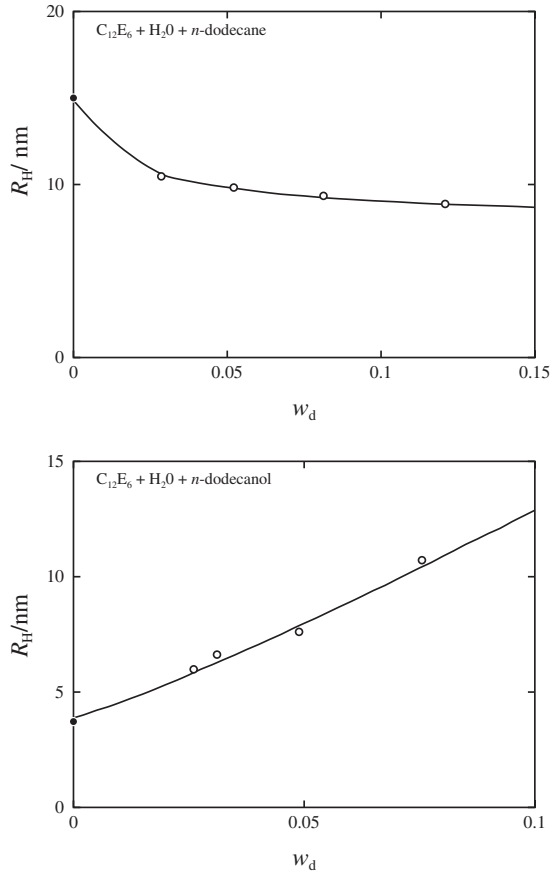

Figure 6. Plots of R_H against w_d for $C_{12}E_6$ + water + *n*-dodecane solutions at 40.0 °C and for $C_{12}E_6$ + water + *n*-dodecanol solutions at 25.0 °C: Unfilled circles, present data; Filled circles, previous results for the $C_{12}E_6$ + water binary system.[15]

ues at $w_d = 0$ (filled circles) are the results for the binary system $C_{12}E_6$ + water obtained previously.[15] Similarly to the w_d dependence of M_w indicated in Figure 4, R_H of the $C_{12}E_6$ + *n*-dodecane micelle decreases with *n*-dodecane content, while that of the $C_{12}E_6$ + *n*-dodecanol micelle increases with *n*-dodecanol content. This again indicates that $C_{12}E_6$ micelles disintegrate with addition of *n*-dodecane, but become larger with the *n*-dodecanol uptake. The former result is similar to literature findings for $C_{12}E_5$ micelles containing dodecane[19] and PI–PEO.[22] As pointed out by Menge *et al.*, the decrease of R_H along with M_w is considered due to a transition from wormlike micelles to microemulsion droplets. The incorporation of *n*-dodecane into the cylindrical micelles may cause increase of micellar diameter and then decrease in hydrophilic interaction among polyoxyethylene tails of $C_{12}E_6$ molecules and solvent water, resulting in decrease of solubility of the micelles. This may explain the disintegration of originally wormlike micelles into smaller droplets. The growth of micellar size with the *n*-dodecanol uptake suggests that *n*-dodecanol functions as co-surfactant in the micelles.

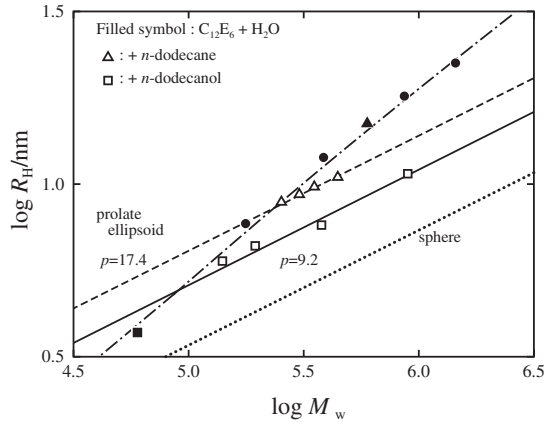

Figure 7. Plots of R_H against M_w for $C_{12}E_6$ + water + *n*-dodecane solutions at 40.0 °C (triangles) and for $C_{12}E_6$ + water + *n*-dodecanol solutions at 25.0 °C (squares): Unfilled symbols, present data; Filled symbols, previous results for $C_{12}E_6$ + water binary system;[15] Various lines indicate the theoretical values calculated different models: chain, wormlike spherocylinder model;[15] dashed, prolate ellipsoid with axial ratio $p = 17.4$; solid, prolate ellipsoid with axial ratio $p = 9.2$; dotted, sphere.

DISCUSSION

To elucidate the shape evolution of the $C_{12}E_6$ micelles caused by *n*-dodecan or *n*-dodecanol uptake, we double-logarithmically plotted R_H against M_w in Figure 7. The data points shown by triangles and squares represent micelles containing *n*-dodecane and *n*-dodecanol with various content w_d. The filled triangle and square denote the value for $w_d = 0$. The various filled symbols denote previous results[15] for the binary system $C_{12}E_6$ + water. The data points are satisfactorily represented by theoretical calculations with the wormlike spherocylinder model[26–28] as indicated by the dot-dashed curve.

Each data set for the micelles in the present two ternary systems approximately follows a straight line with slope 1/3. Thus, the micelles may vary in size without change in shape. We first calculated R_H as a function of M_w assuming a spherical shape of the micelles by

$$R_H = \left(\frac{3vM_w}{4\pi N_A}\right)^{1/3} \tag{11}$$

where v is the partial specific volume of the sphere. The results shown by the dotted line are significantly lower than the observed values of R_H (unfilled triangles and squares), indicating that the micelles are not spherical. Then, we calculated R_H with prolate and oblate ellipsoid models by the equations given as[29]

$$R_H = \frac{R_e(P^2-1)^{1/2}}{P^{1/3}\ln[P+(P^2-1)^{1/2}]} \quad \text{(prolate ellipsoid)} \tag{12}$$

$$R_H = \frac{R_e(P^2-1)^{1/2}}{P^{2/3}\tan^{-1}(P^2-1)^{1/2}} \quad \text{(oblate ellipsoid)} \tag{13}$$

Here P is the axial ratio of the ellipsoid *i.e.*, the major radius divided by the minor one, and R_e is the radius of a sphere equal in volume to the ellipsoid. In turn, R_e is represented as

$$R_e = P^{1/3}b \quad \text{(prolate ellipsoid)} \tag{14}$$

$$R_e = P^{2/3}b \quad \text{(oblate ellipsoid)} \tag{15}$$

with b the minor radius of the ellipsoid. The effective radius R_e of the ellipsoid is related to molar mass M_w as,

$$\frac{4\pi R_e^3}{3} = \frac{M_w v}{N_A} \tag{16}$$

with v the specific volume of the ellipsoid. In theoretical calculations for the sphere and ellipsoids, v is taken to be independent of P in the case of ellipsoid, and equal to observed values of the corresponding micelles. From eqs 12 through 16, R_H for the prolate or oblate ellipsoid is proportional to $M_w^{1/3}$ in line with the present experimental observations, provided that P is independent of M_w.

Calculations with the oblate ellipsoid model at a given M_w afford R_H smaller than calculated with the rigid sphere model, depending on P. Accordingly, only the prolate ellipsoid model, substantially the same as a rigid rod model, may explain the present results for the relationship between R_H and M_w. The micellar shape is analogous to the one inferred by Menge *et al.*[17–19] for $C_{12}E_5$ micelles containing decane. In actuality, calculations with the prolate ellipsoids with $P = 17.4$ and $P = 9.2$ quantitatively explain R_H for $C_{12}E_6$ micelles containing *n*-dodecane and *n*-dodecanol, respectively, as seen in Figure 7. The values of the minor axis b thus determined are summarized in Tables I and II for the $C_{12}E_6$ + *n*-dodecane and $C_{12}E_6$ + *n*-dodecanol micelles, respectively. Shape variation between wormlike micelles and rigid ellipsoidal ones, *i.e.*, between filled and unfilled triangles or filled and unfilled squares, has not been clarified as yet.

From P and b, we calculated the volume V of the individual ellipsoidal micelles and the volume V_1 allotted to each $C_{12}E_6$ molecule (including *n*-dodecane or *n*-dodecanol) in the micelles. In Figure 8, V and V_1 are plotted against w_d. As expected from w_d dependence of M_w depicted in Figure 4, V decreases with w_d following a curve concave upward in the $C_{12}E_6$ + water + *n*-dodecane system, while V increases with w_d in the $C_{12}E_6$ + water + *n*-dodecanol system. V_1 does not significantly change with w_d but somewhat increases linearly with w_d in both systems.

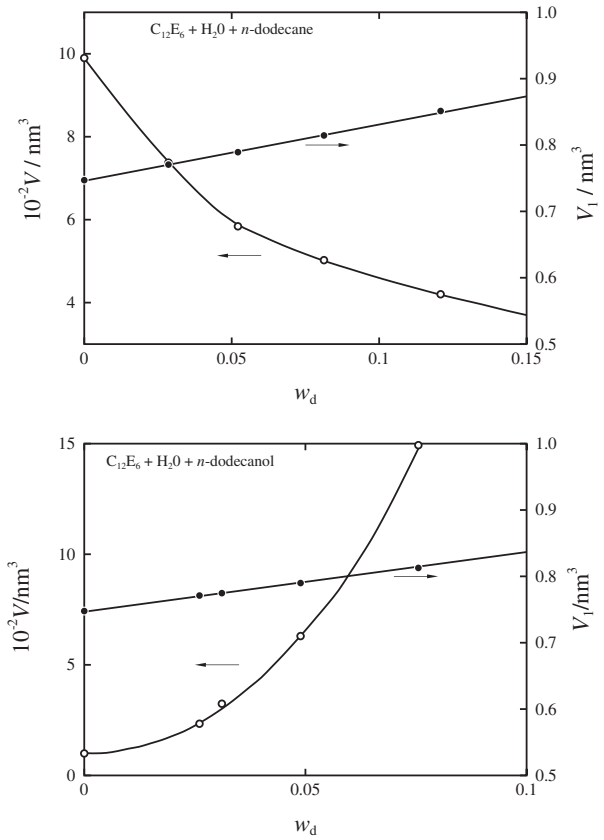

Figure 8. w_d dependence of the micelle volume V and the volume V_1 per $C_{12}E_6$ molecule for $C_{12}E_6$ + water + *n*-dodecane solutions at 40.0 °C and for $C_{12}E_6$ + water + *n*-dodecanol solutions at 25.0 °C. The values at $w_d = 0$ are the previous results for $C_{12}E_6$ + water binary system.[15]

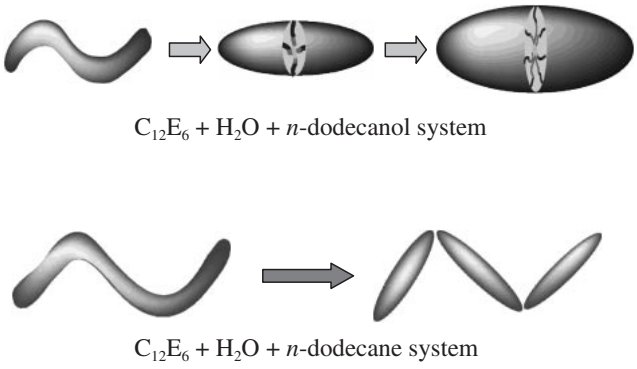

Figure 9. Schematic drawings of variation in shape and size of $C_{12}E_6$ micelles with w_d for $C_{12}E_6$ + water + *n*-dodecane and the $C_{12}E_6$ + water + *n*-dodecanol systems.

Thus, although $C_{12}E_6$ micelles collapse by incorporating with *n*-dodecane and grow in size by including *n*-dodecanol, each $C_{12}E_6$ molecule share inclusions in a similar fashion in both systems.

Figure 9 schematically illustrates variation in shape and size of $C_{12}E_6$ micelles on incooperating the oil component. $C_{12}E_6$ micelles increase in size with *n*-dodecanol uptake, while in the case of *n*-dodecane

as oil the micelles collapse into smalle size. For both systems, change in shape was observed from wormlike micelles to prolate ellipsoids.

CONCLUSIONS

Size and shape variation of $C_{12}E_6$ micelles with oil (*n*-dodecane and/or *n*-dodecanol) uptake was investigated by SLS and DLS measurements. In the characterization, molar mass M_w and hydrodynamic radius R_H of the "isolated" individual micelle were determined from extrapolations of the SLS and DLS data to infinite dilution, thereby eliminating the effects of the intermicellar thermodynamic and hydrodynamic interactions on the basis of the previous results.[15]

$C_{12}E_6$ micelles collapse into smaller ones by incorporating *n*-dodecane and grow to larger ones when *n*-dodecanol is included in them. The former may indicate that the addition of *n*-dodecane into the micelles weakens hydrophilic interactions among polyoxyethylene tails of the $C_{12}E_6$ molecules forming the micelles and the solvent water too significantly to maintain the original micellar size as mentioned by Menge *et al.*[17–19] The latter implies that *n*-dodecanol functions as co-surfactant in the micelles, since it has a hydroxyl group which may work as a hydrophilic group.

Accompanying size change, the micellar shape is altered from the original wormlike shape to prolate ellipsoid with axial ratio of 17.4 and 9.2 with the *n*-dodecane and *n*-dodecanol uptake, respectively. The values of the minor axis decreases in the former and increases in the latter with oil content. The volume shared by each $C_{12}E_6$ molecule (including the added oil) in the micelles does not vary much with oil content, suggesting that arrangement of the surfactant molecules remains unaltered by and large.

Acknowledgment. This research was supported in part by a Grand-in-Aid for Scientific Research (14550849) from the Ministry of Education, Culture, Sports, Science and Technology, Japan.

REFERENCES

1. W. Brown, R. Johnson, P. Stilbs, and B. Lindman, *J. Phys. Chem.*, **87**, 4548 (1983).
2. T. Kato and T. Seimiya, *J. Phys. Chem.*, **90**, 1986 (1986).
3. W. Brown and R. Rymden, *J. Phys. Chem.*, **91**, 3565 (1987).
4. W. Brown, Z. Pu, and R. Rymden, *J. Phys. Chem.*, **92**, 6086 (1988).
5. T. Imae, *J. Phys. Chem.*, **92**, 5721 (1988).
6. W. Richtering, W. Burchard, E. Jahns, and H. Finkelmann, *J. Phys. Chem.*, **92**, 6032 (1988).
7. T. Kato, S. Anzai, and T. Seimiya, *J. Phys. Chem.*, **94**, 7255 (1990).
8. T. M. Kole, C. J. Richards, and M. R. Fisch, *J. Phys. Chem.*, **98**, 4949 (1994).
9. H. Strunk, P. Lang, and G. H. Findenegg, *J. Phys. Chem.*, **98**, 11557 (1994).
10. P. Schurtenberger, C. Cavaco, F. Tiberg, and O. Regev, *Langmuir*, **12**, 2894 (1996).
11. G. Jerke, J. S. Pedersen, S. U. Egelhaaf, and P. Schurtenberger, *Langmuir*, **14**, 6013 (1998).
12. A. Bernheim-Groswasser, E. Wachtel, and Y. Talmon, *Langmuir*, **16**, 4131 (2000).
13. O. Glatter, G. Fritz, H. Lindner, J. Brunner-Papela, R. Mittelbach, R. Strey, and S. U. Egelhaaf, *Langmuir*, **16**, 8692 (2000).
14. T. R. Carale and D. Blankschtein, *J. Phys. Chem.*, **96**, 455 (1992).
15. S. Yoshimura, T. Shirai, and Y. Einaga, *J. Phys. Chem.*, **108**, 15477 (2004).
16. T. Sato, *Langmuir*, **20**, 1095 (2004).
17. U. Menge, P. Lang, and G. H. Findenegg, *J. Phys. Chem. B*, **103**, 5768 (1999).
18. U. Menge, P. Lang, and G. H. Findenegg, *Colloids Surf., A*, **163**, 8 (2000).
19. U. Menge, P. Lang, G. H. Findenegg, and P. Strunz, *J. Phys. Chem. B*, **107**, 1316 (2003).
20. A. Bernheim-Groswasser, T. Tlusty, S. A. Safran, and Y. Talmon, *Langmuir*, **15**, 5448 (1999).
21. H. Kunieda, U. Md. Hemayet, H. Furukawa, and A. Harashima, *Macromolecules*, **34**, 9093 (2001).
22. H. Kunieda, M. Kaneko, M. A. Lopez-Quintela, and M. Tsukahara, *Langmuir*, **20**, 2164 (2004).
23. E. R. Pike, R. M. Pomeroy, and J. M. Vaughan, *J. Chem. Phys.*, **62**, 3188 (1975).
24. Y. Einaga, T. Mitani, J. Hashizume, and H. Fujita, *Polym. J.*, **11**, 565 (1979).
25. G. Briganti, S. Puvvada, and D. Blankschtein, *J. Phys. Chem.*, **95**, 8989 (1991).
26. T. Norisuye, M. Motowoka, and H. Fujita, *Macromolecules*, **12**, 320 (1979).
27. H. Yamakawa and M. Fujii, *Macromolecules*, **6**, 407 (1973).
28. H. Yamakawa and T. Yoshizaki, *Macromolecules*, **12**, 32 (1979).
29. R. F. Probstein, "Physicochemical Hydrodynamics, 2nd ed.," John Willey & Sons, New York, N.Y., 1994.